



# Natural (dihydro)phenanthrene plant compounds are direct activators of AMPK through its allosteric drug and metabolite-binding site

Received for publication, February 1, 2022, and in revised form, March 15, 2022. Published, Papers in Press, March 21, 2022.

<https://doi.org/10.1016/j.jbc.2022.101852>

Matthew J. Sanders<sup>1,\*</sup>, Yann Ratinaud<sup>1</sup>, Katyayane Neopane<sup>1,2</sup>, Nicolas Bonhoure<sup>1</sup>, Emily A. Day<sup>3,4</sup>, Olivier Ciclet<sup>1</sup>, Steve Lassueur<sup>1</sup>, Martine Naranjo Pinta<sup>1</sup>, Maria Deak<sup>1</sup>, Benjamin Brinon<sup>1</sup>, Stefan Christen<sup>5</sup>, Gregory R. Steinberg<sup>3,4</sup>, Denis Barron<sup>1</sup>, and Kei Sakamoto<sup>1,6,\*</sup>

From the <sup>1</sup>Nestlé Institute of Health Sciences, Nestlé Research, Société des Produits Nestlé S.A., Lausanne, Switzerland; <sup>2</sup>School of Life Sciences, Ecole Polytechnique Fédérale de Lausanne (EPFL), Lausanne, Switzerland; <sup>3</sup>Centre for Metabolism, Obesity, and Diabetes Research, and <sup>4</sup>Department of Medicine and Department of Biochemistry and Biomedical Sciences, McMaster University, Hamilton, Ontario, Canada; <sup>5</sup>Nestlé Institute of Food Safety and Analytical Sciences, Nestlé Research, Société des Produits Nestlé S.A., Lausanne, Switzerland; <sup>6</sup>Novo Nordisk Foundation Center for Basic Metabolic Research, University of Copenhagen, Copenhagen, Denmark

Edited by Joseph Jez

AMP-activated protein kinase (AMPK) is a central energy sensor that coordinates the response to energy challenges to maintain cellular ATP levels. AMPK is a potential therapeutic target for treating metabolic disorders, and several direct synthetic activators of AMPK have been developed that show promise in preclinical models of type 2 diabetes. These compounds have been shown to regulate AMPK through binding to a novel allosteric drug and metabolite (ADaM)-binding site on AMPK, and it is possible that other molecules might similarly bind this site. Here, we performed a high-throughput screen with natural plant compounds to identify such direct allosteric activators of AMPK. We identified a natural plant dihydrophenanthrene, Lusianthridin, which allosterically activates and protects AMPK from dephosphorylation by binding to the ADaM site. Similar to other ADaM site activators, Lusianthridin showed preferential activation of AMPK $\beta$ 1-containing complexes in intact cells and was unable to activate an AMPK $\beta$ 1 S108A mutant. Lusianthridin dose-dependently increased phosphorylation of acetyl-CoA carboxylase in mouse primary hepatocytes, which led to a corresponding decrease in *de novo* lipogenesis. This ability of Lusianthridin to inhibit lipogenesis was impaired in hepatocytes from  $\beta$ 1 S108A knock-in mice and mice bearing a mutation at the AMPK phosphorylation site of acetyl-CoA carboxylase 1/2. Finally, we show that activation of AMPK by natural compounds extends to several analogs of Lusianthridin and the related chemical series, phenanthrenes. The emergence of natural plant compounds that regulate AMPK through the ADaM site raises the distinct possibility that other natural compounds share a common mechanism of regulation.

Natural plant compounds have traditionally been used in herbal medicine for centuries for the treatment or prevention of a variety of human diseases. Some of these natural products are being assessed in clinical trials or have been used as lead compounds, modified to improve efficacy and bioavailability, to generate clinically relevant compounds (1–4). Interestingly, a plethora of natural plant polyphenols, including resveratrol, quercetin, and berberine, have been shown to activate the energy-sensing enzyme, AMP-activated protein kinase (AMPK), raising the possibility that some of their beneficial effects may be mediated by activation of AMPK (5, 6). Therefore, the potential role of AMPK in mediating the health benefits of natural compounds and antidiabetic drugs has stimulated interest in this enzyme as a therapeutic target for treating various metabolic disorders.

AMPK is an evolutionary conserved Ser/Thr protein kinase and functions to control cellular and whole-body energy homeostasis (7, 8). AMPK is a heterotrimeric complex consisting of a catalytic  $\alpha$  subunit and regulatory  $\beta$  and  $\gamma$  subunits, and multiple isoforms exist for each subunit ( $\alpha$ 1,  $\alpha$ 2,  $\beta$ 1,  $\beta$ 2,  $\gamma$ 1,  $\gamma$ 2, and  $\gamma$ 3) allowing for 12 AMPK complexes. The  $\alpha$  catalytic subunit contains an N-terminal kinase domain, which when phosphorylated in a conserved activation loop (site Thr172) by upstream kinases (liver kinase B1 and calcium/calmodulin-dependent protein kinase kinase 2 [CaMKK2]) becomes activated (7, 9). The activated (Thr172-phosphorylated) form of AMPK can be maintained by the binding of AMP or ADP to the cystathionine  $\beta$ -synthase domains of the  $\gamma$  subunit (10, 11). Furthermore, AMP can increase AMPK activity further through an allosteric mechanism (12). In contrast, ATP antagonizes the effects of AMP and ADP, and this forms the basis by which AMPK can respond to fluctuations in the AMP:ATP and ADP:ATP ratios during times of energy demand and maintains ATP at a constant level.

Natural/naturally derived plant compounds, metformin and canagliflozin, were shown to activate AMPK as a consequence

\* For correspondence: Matthew J. Sanders, [matthew.sanders@rd.nestle.com](mailto:matthew.sanders@rd.nestle.com); Kei Sakamoto, [kei.sakamoto@sund.ku.dk](mailto:kei.sakamoto@sund.ku.dk).

## Natural plant compounds directly regulate AMPK

of their ability to inhibit mitochondrial ATP production, altering the AMP/ADP:ATP ratio and thus activate AMPK through nucleotide binding to the  $\gamma$  subunit (13, 14). Interestingly, this mechanism for activation of AMPK is currently being exploited to develop compounds that “mimic” the effects of exercise or metformin by inhibiting mitochondrial respiration (15, 16). However, because of the fact that metformin, canagliflozin, and natural plant compounds indirectly activate AMPK, it is likely that these compounds have a combination of AMPK-dependent and AMPK-independent effects (6). For example, some of the effects of metformin may be the result of modulating redox-dependent mechanism (17) or other nucleotide-regulated enzymes, including fructose-1,6-bisphosphatase 1 (18, 19).

In contrast to natural products that activate AMPK by inhibiting mitochondrial respiration and disrupting the homeostatic AMP/ADP:ATP ratio, the natural plant compound salicylic acid, the active component of aspirin, activates AMPK through a distinct mechanism (20, 21). The authors reported that some of the beneficial effects of salicylic acid on lipid homeostasis may be mediated by activation of AMPK (20, 22); however, indirect effects on mitochondrial proton gradient have also been reported (23). Importantly, salicylic acid is being assessed in clinical trials for treating type 2 diabetes and cardiovascular disease (24, 25). Whilst at high concentrations, salicylic acid was shown to alter the ADP:ATP ratio of the cell, at lower concentrations, salicylic acid activated an AMP-insensitive AMPK mutant ( $\gamma$ 2 R531G) in cells (20). Instead, salicylic acid-induced activation of AMPK was blunted by a  $\beta$ 1 S108A AMPK mutant (20), which has previously been shown to alter the activation of AMPK by synthetic small-molecule activators, including A-769662 and 991 (26, 27).

A-769662, a member of the thienopyridone family, was the first direct activator of AMPK to be identified (28) that appeared to regulate AMPK independent of the nucleotide-binding site (26, 29, 30). Subsequently, several studies identified similar direct AMPK activators such as 991 (a benzimidazole derivative) and showed that they share a common mechanism of action (6). Through this research, a novel regulatory site was identified (27) separate from the canonical nucleotide-binding site in the  $\gamma$  subunit. This site, termed the allosteric drug and metabolite (ADaM)-binding site, is formed at the interface between the N-lobe of the  $\alpha$  kinase domain and the carbohydrate-binding module (CBM) of the  $\beta$  subunit (27, 31). Consequently, pharmaceutical companies have been using this novel regulatory site to develop potent selective direct synthetic activators of AMPK (6, 32). Some of these compounds have shown *in vivo* efficacy and display beneficial effects in rodent and nonhuman primate models of type 2 diabetes (33, 34) and more recently in rodent models with nonalcoholic steatohepatitis (35). These studies suggest that direct activation of AMPK by targeting the ADaM-binding site is a viable approach for treating metabolic disorders.

The identification of the ADaM site as a novel regulatory site on AMPK has raised the possibility that endogenous natural metabolite(s) may regulate AMPK. A recent publication reported that long-chain fatty acyl-CoAs may act as

endogenous direct AMPK activators (36). In addition, the demonstration that salicylic acid binds and regulates AMPK through the ADaM site (20, 31) raises an intriguing possibility that other naturally occurring compounds may also regulate AMPK through this site. In this study, we identified natural pure compounds from two chemical classes, phenanthrenes and dihydrophenanthrenes, which directly activate AMPK through the ADaM-binding pocket. These compounds increase AMPK activity in intact cells and show dose-dependent inhibition of *de novo* lipogenesis in primary hepatocytes. The ability of these compounds to inhibit hepatic lipogenesis was impaired by the AMPK $\beta$ 1 S108A knock-in (KI) mutation in the ADaM-binding site and mutation of the AMPK phosphorylation site in the substrate acetyl-CoA carboxylase 1/2 (ACC1/2). The identification of dihydrophenanthrenes and phenanthrenes, in addition to the previously reported salicylic acid, suggests that activation of AMPK through the ADaM site could represent a common mechanism for natural plant compounds to regulate AMPK. This study provides growing evidence that natural compounds can regulate AMPK and supports the concept that an endogenous mammalian natural metabolite may bind to the ADaM site and activate AMPK.

## Results

### High-throughput screening of a natural bioactive library identifies Lusianthridin as a direct activator of AMPK

To identify pure natural compounds or extracts that directly activate AMPK, we performed a high-throughput screen of a panel of natural bioactives (around 42,000 pure compounds, extracts, and fractions) using the Homogenous Time-Resolved Fluorescence (HTRF) KinEASE STK assay (37) and monitored allosteric activation of recombinant human AMPK $\alpha$ 2 $\beta$ 1 $\gamma$ 1 complex. We identified that Lusianthridin (Chemical Abstracts Service [CAS] registry number: 87530-30-1, Fig. 1A), a dihydrophenanthrene, is a direct allosteric activator of recombinant AMPK with a similar EC<sub>50</sub> (~10  $\mu$ M) and fold activation compared with AMP (Fig. 1B). Hit confirmation was carried out on a sample prepared by chemical synthesis, and we show that there is comparable allosteric activation to the natural Lusianthridin from the initial screening library (Fig. 1C). The identity of all the Lusianthridin samples was confirmed by our quality control analyses (Fig. S1).

To determine whether Lusianthridin mediated its effects through the same binding site as AMP, recombinant AMPK $\alpha$ 2 $\beta$ 1 $\gamma$ 1 was incubated with varying concentrations of AMP in the absence or the presence of fixed concentrations of Lusianthridin. As shown in Figure 1D, incubation of AMPK with AMP in the presence of its analog 5-aminoimidazole-4-carboxamide-1-D-ribofuranosyl-5'-monophosphate did not lead to a further increase in allosteric activation, consistent with the ability of 5-aminoimidazole-4-carboxamide-1-D-ribofuranosyl-5'-monophosphate to bind to the same binding pocket as AMP in the  $\gamma$  subunit of AMPK. In contrast, A-769662, which binds to the ADaM site, resulted in an enhancement in AMP allosteric activation (Fig. 1E). Interestingly, Lusianthridin also enhanced AMP allosteric activation,

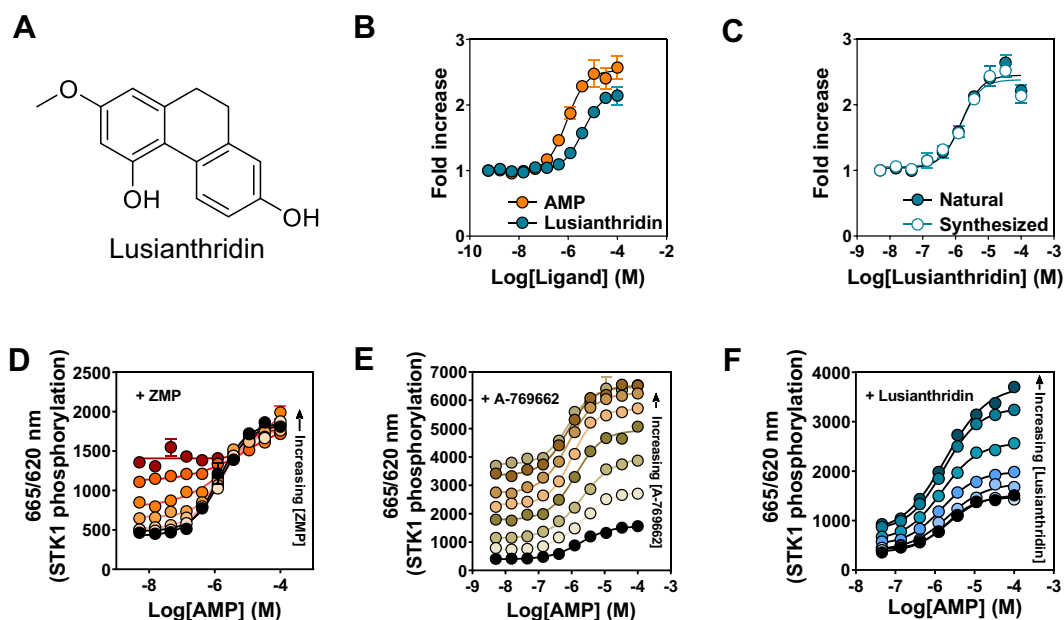


**Figure 1. Identification of Lusianthridin as a direct activator of AMPK.** A, structure of Lusianthridin. B, AMPK activity of bacterially expressed recombinant human  $\alpha 2\beta 1\gamma 1$  complex in the presence of increasing concentrations of AMP or Lusianthridin. C, comparison of Lusianthridin isolated from a natural source and Lusianthridin generated by chemical synthesis. AMPK activity was determined using the HTRF KinEASE assay kit, and results are presented as fold increase in AMPK activity ( $\pm$ SEM,  $n = 3$ ) relative to the activity in the absence of activator. D–F, recombinant  $\alpha 2\beta 1\gamma 1$  was incubated with increasing concentrations of AMP in the absence (black circles) or the presence of fixed concentrations of ZMP (D) (1.23–300  $\mu$ M), Lusianthridin (E) (0.137–100  $\mu$ M), or A-769662 (F) (0.014–10  $\mu$ M). The increasing concentrations are indicated on the graph by the arrow and represented by a different color. AMPK activity was determined using the HTRF KinEASE assay kit, and results are presented as the ratio of 665/620 nm (STK1 substrate peptide phosphorylation). AMPK, AMP-activated protein kinase; HTRF, Homogenous Time-Resolved Fluorescence; ZMP, 5-aminoimidazole-4-carboxamide-1-D-ribofuranosyl-5'-monophosphate.

suggesting that Lusianthridin activates AMPK through a distinct binding site to AMP (Fig. 1F).

#### Lusianthridin activates AMPK through the ADaM site

It is possible to distinguish ligands that regulate AMPK at the two distinct regulatory sites on AMPK by their activity profile against various AMPK complexes with mutations in either the  $\beta$  or  $\gamma$  subunits (13, 20). As seen in Figure 2, A and B, in contrast to AMP, Lusianthridin activates AMPK complexes harboring a  $\gamma 1$  Arg to Gly mutation at residue 299 (R299G), to the same extent as WT AMPK $\alpha 2\beta 1\gamma 1$  complexes. In contrast, Lusianthridin did not activate  $\alpha 2\beta 1\gamma 1$  complexes with a mutation at Ser108 to Ala in the  $\beta 1$  subunit (S108A), and a truncation at residue  $\beta 1$  186 that removes the N-terminal CBM, thus this mutant is termed as  $\Delta$ CBM (Fig. 2A). This activity profile is characteristic of direct activators at the ADaM-binding site as we also show here with the benchmark compound, A-769662 (Fig. 2C). Consistent with this, we did not detect Lusianthridin-stimulated allosteric activation of  $\beta 2$ -containing AMPK complexes ( $\alpha 2\beta 2\gamma 1$ ), which fits with our current knowledge that vast majority of the ADaM-site ligands, but not all (38), have no or an impaired activity profile against  $\beta 2$ -containing complexes (6, 27, 39) (Fig. S2).

We tested Lusianthridin (10  $\mu$ M) in a cell-free assay against a panel of 140 human protein kinases to probe the specificity of this compound for AMPK. Lusianthridin did not robustly activate (>25%) any kinases in the panel, with most kinases showing no significant alteration in their activity (Fig. S3). AMPK was not activated by Lusianthridin since the recombinant AMPK protein used in the kinase panel was

$\beta 2$ -containing complex (AMPK $\alpha 1\beta 2\gamma 1$ ). Lusianthridin appeared to decrease the activity of a small subset of kinases, however, with a number of those displayed over a 50% reduction in activity (the proviral integration site for Moloney murine leukemia virus 1 and dual-specificity tyrosine-regulated kinase families). These kinases were reported to be inhibited by several compounds (40) (Kinase Profiling Inhibitor Database, <http://www.kinase-screen.mrc.ac.uk/kinase-inhibitors>) and are also inhibited by A-769662 (29). These data indicate that Lusianthridin is not a promiscuous allosteric activator of protein kinases.

In addition to allosteric activation, we show that Lusianthridin also caused a dose-dependent protection against dephosphorylation of AMPK by protein phosphatase 2 $\alpha$  (PP2C $\alpha$ ) in a cell-free assay (Fig. 2, D–F). Interestingly, similar to A-769662, Lusianthridin displayed impaired protection against dephosphorylation of the AMPK $\alpha 2\beta 1$ (S108A) $\gamma 1$  mutant, whereas the effects of AMP are largely unaffected by this mutation. Taken together, our *in vitro* data demonstrate that Lusianthridin regulates AMPK through the ADaM-binding pocket similar to synthetic direct activators, including A-769662.

#### Lusianthridin increases AMPK activity in intact cells

To examine the effects of Lusianthridin in intact cells, we used the human osteosarcoma U2OS cell line to monitor activation of AMPK itself by determining the level of phosphorylation on AMPK $\alpha$  Thr172 and phosphorylation of an established *bona fide* substrate, ACC. These effects were routinely quantified using Western blot analysis using the LI-

## Natural plant compounds directly regulate AMPK

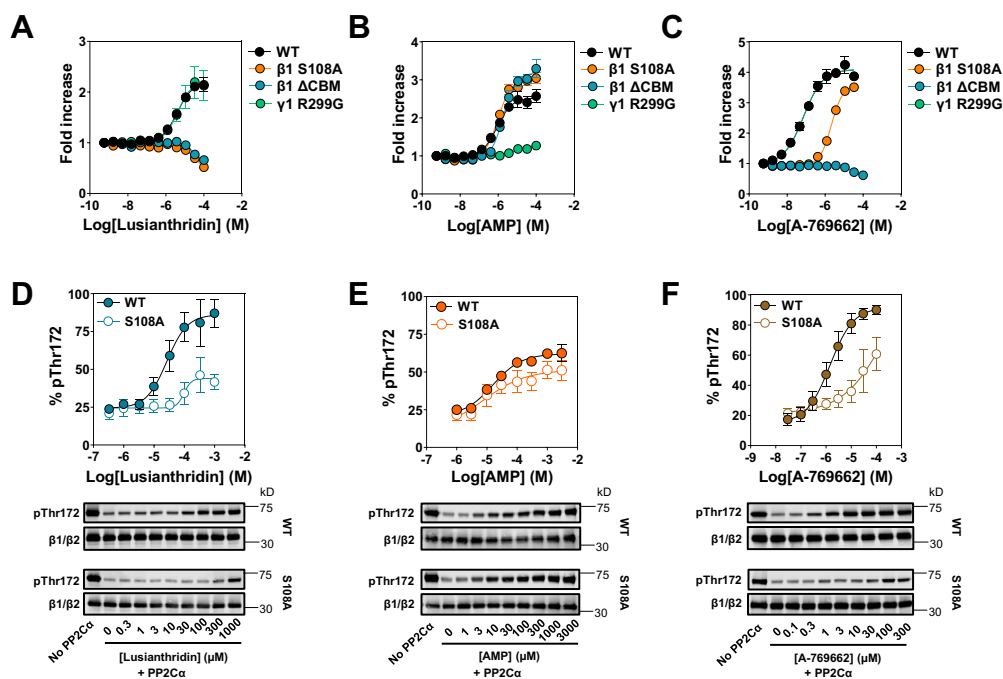


**Figure 2. Effects of Lusianthridin, AMP, or A-769662 on activation and protection from dephosphorylation of various AMPK mutant complexes.** A–C, activation of various AMPK mutant complexes by Lusianthridin, AMP, or A-769662 determined using the HTRF KinEASSE assay kit and displayed as the fold increase in AMPK activity ( $\pm$ SEM,  $n = 3$ ). D–F, increasing concentrations of Lusianthridin (D), AMP (E), or A-769662 (F) were incubated with phosphorylated (Thr172)  $\alpha 2\beta 1\gamma 1$  WT or  $\alpha 2\beta 1\gamma 1$  S108A (S108A) in the presence of protein phosphatase 2Ca (PP2Ca) for 10 min at 30 °C. Phosphorylation of AMPK $\alpha$  was determined by Western blot analysis using the anti-phospho-Thr172 antibody. Phosphorylation was quantified and is displayed above a representative Western blot image and is the means  $\pm$  SEM of at least three independent experiments. AMPK, AMP-activated protein kinase; HTRF, Homogenous Time-Resolved Fluorescence.

COR Odyssey system. Furthermore, we also used a phospho-ACC (Ser79) cellular HTRF assay kit (96-well plate reader assay format), which we optimized for this cell line to measure activation of AMPK in a linear range across a number of doses of compounds, including A-769662 and an AMP mimetic prodrug, 5-aminoimidazole-4-carboxamide riboside (AICAR) (Fig. 3A). Importantly, the ability of these compounds to stimulate increases in phospho-ACC was comparable between our Western blot analysis and HTRF assay (Fig. S4, A–C); therefore, in some experiments, the HTRF assay was solely used to monitor activation of AMPK in cells. Treatment of cells with Lusianthridin increased phospho-ACC in a dose-dependent manner (Fig. 3, A and B), with an improved dose–response compared with salicylic acid (Fig. S4D). We observed that Lusianthridin stimulated phospho-ACC after incubation for 30 min, and this activity was maintained up to the maximum time point tested in this study (4 h) (data not shown). We were able to rule out that increases in  $[Ca^{2+}]_i$  were mediating Lusianthridin-induced increases in AMPK activity through CaMKK2. Preincubation with the CaMKK2 inhibitor STO-609 (41, 42) did not affect the dose–response of Lusianthridin (Fig. 3C), whereas as expected, it impaired ionomycin-mediated activation of AMPK (Fig. S5).

We generated a single  $\beta 1$  knock-out (KO) in U2OS cells to monitor the dependency of ADaM-site activators for  $\beta 1$ -containing complexes.  $\beta 1$  deletion resulted in not only a decrease in overall AMPK $\alpha$  expression but also a modest increase in  $\beta 2$ -isoform expression presumably to compensate for the loss of  $\beta 1$  in these cells (Fig. S6). Importantly, despite the

lower AMPK $\alpha$  expression and corresponding decrease in basal phospho-ACC in these cells (Fig. S6), AICAR caused a dose-dependent increase in phospho-ACC in both the U2OS parental (WT) and  $\beta 1$  KO cells, with a comparable  $EC_{50}$  (Fig. 4A). A-769662, which has previously been reported to be almost entirely  $\beta 1$  specific in intact cells (30), displayed an almost complete ablation of its ability to increase phospho-ACC in the  $\beta 1$  KO cells (Fig. 4B). Similarly, Lusianthridin stimulation of phospho-ACC was almost completely abrogated in the  $\beta 1$  KO cells (Fig. 4, C and D), consistent with our *in vitro* data showing that Lusianthridin does not allosterically activate recombinant AMPK $\beta 2$ -containing complexes (Fig. S2B).

### Lusianthridin increases ACC phosphorylation in cells through activation of AMPK at the ADaM site

Next, we established a cellular model to monitor the contribution of the ADaM-regulatory site in mediating the cellular effects of AMPK in response to treatment with Lusianthridin and other AMPK activators. To achieve this, we generated a  $\beta 1\beta 2$  double KO (DKO) U2OS cell line (Fig. S7). We took advantage of the Flp-In T-Rex system in our AMPK $\beta$  DKO cell lines to reintroduce and stably express the  $\beta 1$ -WT or  $\beta 1$ -S108A mutant or the  $\beta 2$ -WT or  $\beta 2$ -S108A mutant. Importantly, we were able to generate stable cell lines whereby the expression of the  $\beta 1$  or  $\beta 2$  was comparable, and the  $\alpha$  subunit expression was restored to a similar level compared with the U2OS Flp-In T-Rex parental cells (Fig. 5A). First, we confirmed that AICAR stimulated phospho-ACC to a similar

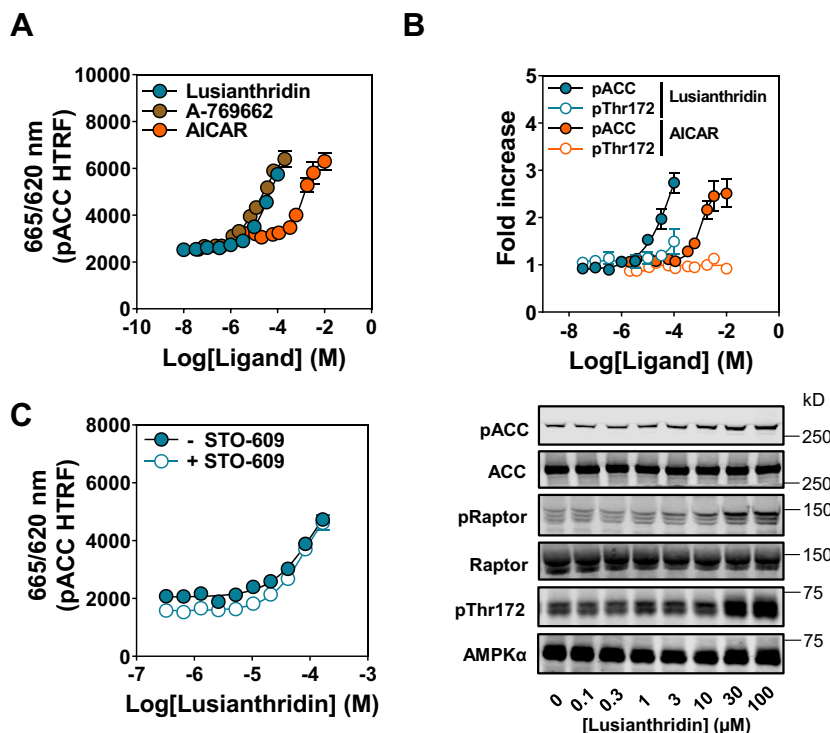


**Figure 3. Effects of Lusianthridin in intact cells.** A, U2OS cells were treated with Lusianthridin, AICAR, or A-769662 for 30 min before lysing and performing an HTRF assay with the phospho-ACC (pACC) assay kit, and results are presented as the ratio of 665/620 nm (pACC HTRF). B, Western blot analysis of U2OS cells treated with Lusianthridin or AICAR with the indicated antibodies. Representative blots of  $n = 3$  are shown along with the quantification of the pACC and pThr172 antibodies. C, U2OS cells were treated with varying concentrations of Lusianthridin for 30 min with or without prior treatment with STO-609 (10  $\mu\text{g}/\text{ml}$ , 1 h). pACC was determined by performing an HTRF assay with the pACC assay kit, and results are presented as the ratio of 665/620 nm (pACC HTRF). A representative blot is displayed for the ionomycin-treated cell lysates using an automated capillary immunoblotting system (Sally Sue). AICAR, 5-aminoimidazole-4-carboxamide riboside; HTRF, Homogenous Time-Resolved Fluorescence.

extent in these genetically engineered new stable cell lines (Fig. 5B), despite the fact that we observed a small decrease in basal AMPK activity because of mutation of  $\beta 1$  S108A compared with WT complexes as previously reported (26) (Fig. S8). Notably, AICAR caused a greater fold increase in maximal response in the  $\beta 2$ -WT-expressing cells compared with the  $\beta 1$ -WT-expressing cells. Interestingly, as shown in Figure 4A, AICAR also caused a greater fold increase in activation of AMPK in the  $\beta 1$ -KO cells, suggesting that  $\beta 2$ -containing complexes appear to be more responsive to AICAR in U2OS cells. In contrast to AICAR, the dose-responses for A-769662 were impaired in both the  $\beta 1$ -S108A and  $\beta 2$ -S108A mutants and  $\beta 2$ -WT cells consistent with this compound regulating AMPK through the ADaM site (Figs. 5C and S8, B and C). Similarly, we show in the  $\beta 1$ -S108A and  $\beta 2$ -S108A mutant and  $\beta 2$ -WT cell lines that Lusianthridin induced increases in phospho-ACC were blunted (Fig. 5, D and E). These data demonstrate that the ability of Lusianthridin to increase AMPK activity in these cells is mainly driven by regulation through the ADaM site of  $\beta 1$ -containing complexes.

#### Lusianthridin inhibits hepatic lipogenesis in an AMPK-dependent manner

We next assessed the ability of Lusianthridin to activate AMPK in a more physiologically relevant cell system. We isolated hepatocytes from C57BL/6 WT mice and treated these

cells with various AMPK activators. We first monitored AICAR-induced activation of AMPK by assessing phosphorylation of ACC in these cells, which inhibits hepatic lipogenesis (43). AICAR caused a robust dose-dependent increase in phosphorylation of ACC and a corresponding dose-dependent inhibition of lipogenesis (Fig. 6A). Lusianthridin also caused a dose-dependent decrease in lipogenesis that correlates closely with the rate of increase in ACC phosphorylation in primary hepatocytes (Fig. 6B). To rule out the possibility that inhibition of lipogenesis by Lusianthridin could be explained by cytotoxicity, we performed a colorimetric 3-[4,5-dimethylthiazol-2-yl]-2,5 diphenyl tetrazolium bromide (MTT) cell viability assay. Under conditions where we observed cytotoxicity with a known cytotoxic agent, carbonyl cyanide 4-(trifluoromethoxy) phenylhydrazone (FCCP, an inhibitor of mitochondrial ATP synthesis), we did not observe any changes in cell viability with treatment of hepatocytes with Lusianthridin (up to 100  $\mu\text{M}$ ) used in this study (Fig. S9).

To determine whether the ability of Lusianthridin to increase phospho-ACC, and inhibit hepatic lipogenesis, was dependent on AMPK, primary mouse hepatocytes were isolated from WT and ACC1/2 double KI (ACC DKI) mice (43). ACC DKI mice have an alanine mutation at the serine residue (ACC1 Ser79Ala/ACC2 Ser212Ala) that is phosphorylated by AMPK. This means that AMPK is not able to phosphorylate and inhibit ACC, and thus, activation of AMPK does not lead to a decrease in lipogenesis (43). We observed that

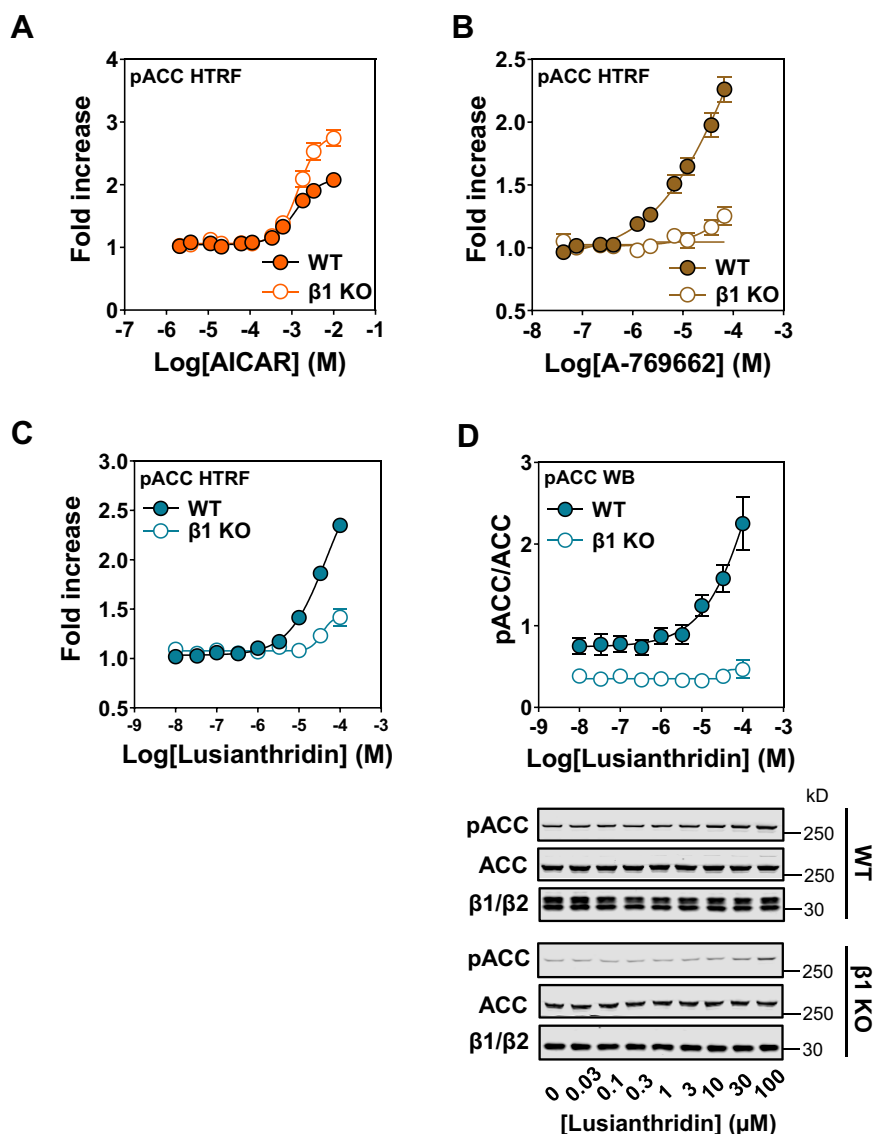


**Figure 4. Effects of Lusianthrudin in  $\beta 1$  KO U2OS cells.** pACC HTRF analysis of WT and  $\beta 1$  KO cells treated with AICAR (A), A-769662 (B), or Lusianthrudin (C). Results are presented as the fold increase in pACC HTRF signal, means  $\pm$  SEM of three independent experiments. D, Western blot (WB) analysis of WT and  $\beta 1$  KO cells treated with Lusianthrudin using the indicated antibodies. Quantification of three independent experiments is shown as a ratio of the signal of pACC/ACC, along with a representative blot. AICAR, 5-aminoimidazole-4-carboxamide riboside; HTRF, Homogenous Time-Resolved Fluorescence; pACC, phospho-ACC.

Lusianthrudin (20 and 40  $\mu\text{M}$ ) and A-769662 (10  $\mu\text{M}$ ) were ineffective at suppressing lipogenesis in primary hepatocytes taken from ACC DKI mice, suggesting that regulation of lipogenesis by these compounds is dependent on AMPK-mediated phosphorylation of ACC (Fig. 6C). Taken together, we demonstrate that Lusianthrudin can activate AMPK in a physiologically relevant cell system and leads to the inhibition of hepatic *de novo* lipogenesis in an AMPK-dependent manner.

#### Lusianthrudin activates AMPK in primary mouse hepatocytes through the ADaM site

Given the importance of the  $\beta 1$  S108 residue in mediating the regulation of AMPK by ADaM-site activators (20, 26, 27), we generated KI mice with an AMPK $\beta 1$  S108A (S108A KI)

mutation in order to assess the contribution of the ADaM site in the regulation of AMPK. We isolated hepatocytes from WT and S108A KI mice to investigate the contribution of the ADaM site in the regulation of lipogenesis by AMPK activators. First, we measured AMPK signaling in WT and S108A KI hepatocytes after treatment with AICAR or Lusianthrudin. As shown in Figure 6D, we observed that AICAR increased phospho-ACC to a similar extent in the WT and S108A KI hepatocytes, whereas Lusianthrudin displayed impaired AMPK signaling (judged by phospho-ACC) in the S108A KI hepatocytes (Fig. 6E). Next, we measured the effect of these compounds on lipogenesis in the S108A KI hepatocytes. First, we observed an increase in basal lipogenesis in hepatocytes isolated from S108A mice compared with WT mice (WT, 7.56  $\pm$  0.89 nmol/h/mg versus S108A, 11.77  $\pm$  1.03 nmol/h/mg), consistent with a decrease in basal AMPK activity in primary

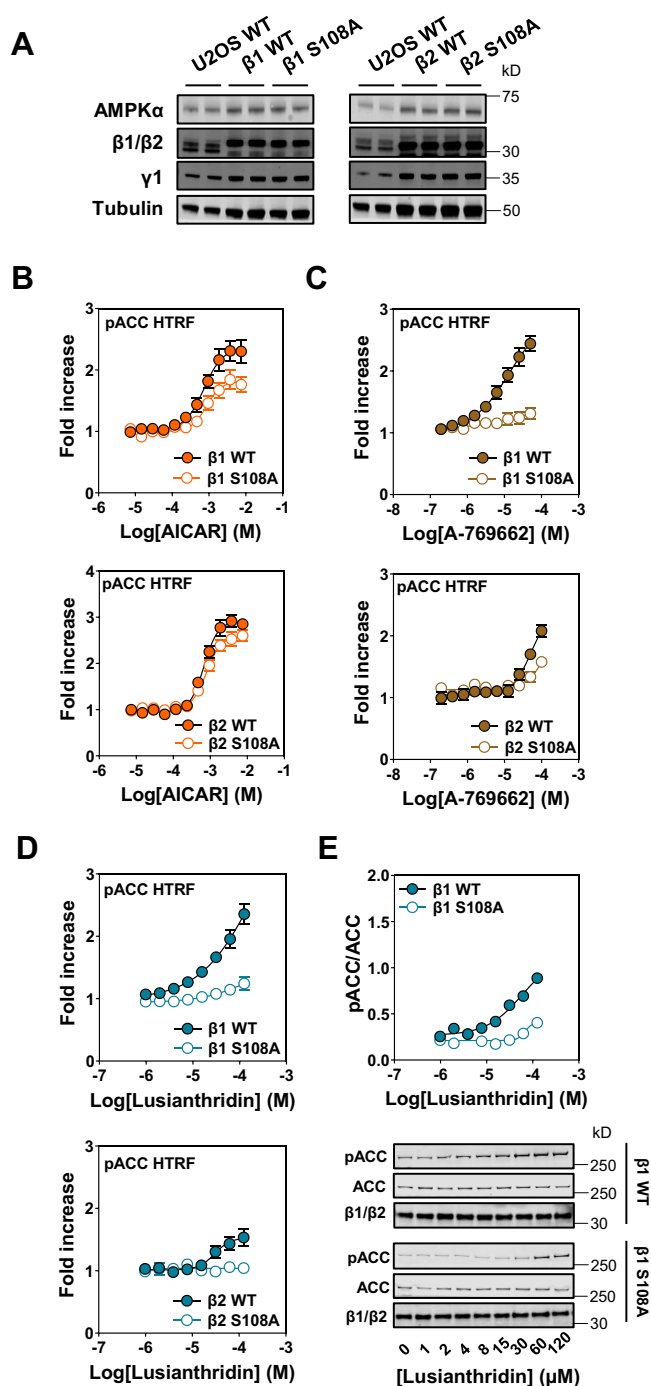


**Figure 5. Effects of Lusianthridin in  $\beta 1/2$  double KO (DKO) U2OS cells stably expressing  $\beta 1$  or  $\beta 2$  WT and  $\beta 1$  or  $\beta 2$  S108A.** A, Western blot analysis of  $\beta 1/2$  DKO cells stably expressing  $\beta 1$  or  $\beta 2$  WT and  $\beta 1$  or  $\beta 2$  S108A using the indicated antibodies. B–D, pACC HTRF analysis of stable cell lines expressing  $\beta 1$  or  $\beta 2$  WT and  $\beta 1$  or  $\beta 2$  S108A treated with AICAR (B), A-769662 (C), or Lusianthridin (D). Results are presented as the fold increase in pACC HTRF signal and are means  $\pm$  SEM of at least three independent experiments. E, Western blot analysis of  $\beta 1$  WT and  $\beta 1$  S108A stable cell lines treated with Lusianthridin using the indicated antibodies. Quantification of three independent experiments is shown as a ratio of the signal of pACC/ACC, along with a representative blot. AICAR, 5-aminoimidazole-4-carboxamide riboside; HTRF, Homogenous Time-Resolved Fluorescence; pACC, phospho-ACC.

hepatocytes and cell culture with this mutation. Despite this, importantly, we demonstrate the ability of AICAR to increase phospho-ACC to a similar extent in WT and S108A KI

hepatocytes, and thus, we observed a comparable inhibition of lipogenesis in these hepatocytes (Fig. 6F). In conjunction with impaired phosphorylation of ACC in S108A KI hepatocytes treated with Lusianthridin, we observed a diminished ability of Lusianthridin to inhibit lipogenesis in these hepatocytes (Fig. 6F). These data are consistent with our *in vitro* and cellular work showing that Lusianthridin mediates its effects largely through binding to the ADaM site.

**Phenanthrenes also directly activate AMPK through the ADaM-binding site**

The identification of Lusianthridin as a direct activator of AMPK led us to test various analogs of this natural phytochemical compound. We identified a number of dihydrophenanthrene analogs that lead to direct activation of AMPK $\alpha 2\beta 1\gamma 1$  in the cell-free assay, and this work allowed us to perform a structure–activity relationship study in parallel. In addition, we showed that Lusianthrin (Fig. 7A), the corresponding phenanthrene analog of Lusianthridin, directly allosterically activated AMPK $\alpha 2\beta 1\gamma 1$  almost identically to Lusianthridin (Fig. 7B). We show using our  $\beta 1$ -WT,  $\beta$ -S108A,  $\beta 2$ -WT, and  $\beta 2$ -S108A U2OS stable cell lines that Lusianthrin activation of AMPK in cells is primarily achieved through its ability to bind to the ADaM-binding site (Fig. 7, C and D). Taken together, we show that activation of AMPK by natural compounds extends beyond Lusianthridin and includes a number of its analogs in the dihydrophenanthrene and the phenanthrene series, suggesting that there is a common mechanism for some natural plant chemical families to activate AMPK through the ADaM site.

**Discussion**

There are numerous natural plant compounds that have been shown to activate AMPK (5, 6), and some of these compounds exert beneficial metabolic effects. However, because of the fact that most of these natural bioactives have been demonstrated to indirectly activate AMPK through alterations in the AMP:ATP and ADP:ATP ratios *via* inhibition of mitochondrial respiration (13), it has been suggested that these compounds will likely have a combination of “AMPK-mediated” and “AMPK-independent” effects. In fact, most of the natural compounds that activate AMPK are antifungal and antimicrobial agents that are produced in response to infection (5), and therefore, AMPK activation is expected to be a byproduct of their toxic nature. Salicylic acid, a natural compound from willow bark, not only directly activates AMPK through the ADaM-binding site (20, 31) but also perturb the levels of ATP within the cell at high concentrations (23), characteristic of the expected mechanism of action of most natural compounds. This raises the possibility that other naturally occurring compounds may also activate AMPK directly.

In this study, we used a library of natural compounds to screen for direct allosteric activators of AMPK and identified Lusianthridin, a dihydrophenanthrene, which directly activated the human AMPK $\alpha 2\beta 1\gamma 1$  complex. There are two key

## Natural plant compounds directly regulate AMPK

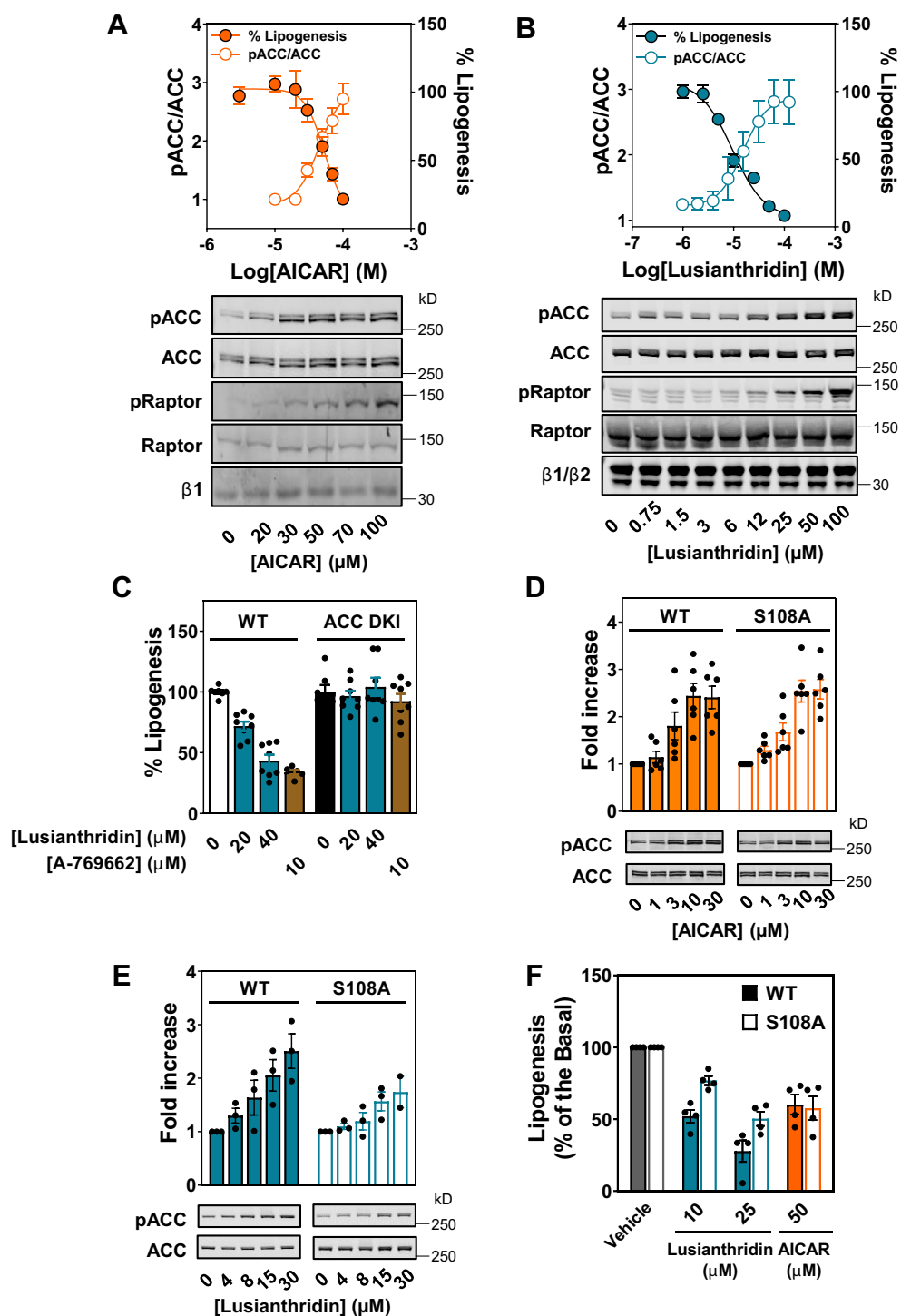


**Figure 6. Lusianthridin activates pACC and inhibits *de novo* lipogenesis in primary mouse hepatocytes.** Dose-dependent inhibition of *de novo* lipogenesis by AICAR (A) or Lusianthridin (B) after treatment of hepatocytes for 1 h. Western blot analysis of hepatocytes treated with AICAR or Lusianthridin is shown under the graph. Quantification of pACC/ACC ratio is displayed on the left Y-axis along with the percentage lipogenesis on the right Y-axis as the mean  $\pm$  SEM from at least three independent experiments. C, inhibition of *de novo* lipogenesis in mouse primary hepatocytes isolated from WT or ACC1 (S79A)/2 (S212A) double KI mice (ACC DK1). Results are displayed as a percentage of lipogenesis and are the mean  $\pm$  SEM from at least two independent experiments. D and E, Western blot analysis of mouse primary hepatocytes isolated from WT or S108A KI (S108A) mice after treatment with the indicated concentrations of AICAR (D) or Lusianthridin (E). Phosphorylation of ACC was quantified and normalized to total ACC protein (pACC/ACC). The fold increase (mean  $\pm$  SEM) in pACC/ACC is displayed above a representative blot of at least three independent experiments. F, inhibition of lipogenesis was determined in WT or S108A KI hepatocytes treated with the indicated concentrations of Lusianthridin or AICAR. Results are displayed as a percentage of lipogenesis and are the mean  $\pm$  SEM from at least three independent experiments. AICAR, 5-aminoimidazole-4-carboxamide riboside; pACC, phospho-ACC.

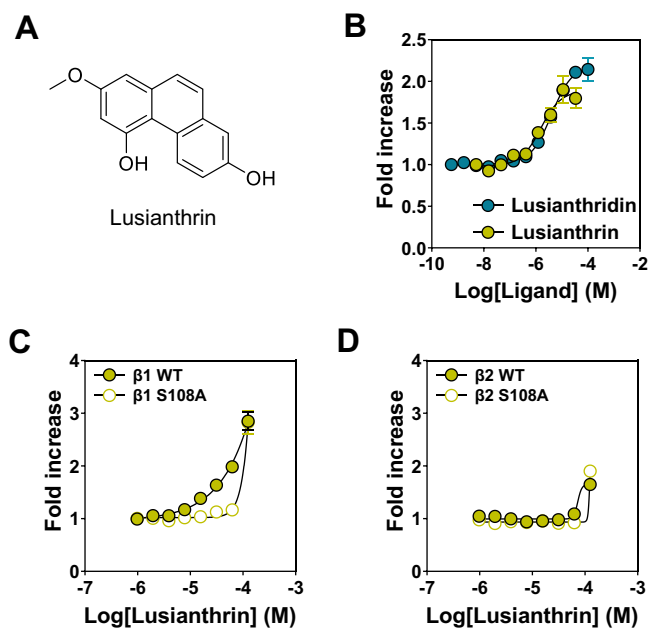


**Figure 7. The phenanthrene, Lusianthridin, also directly activates AMPK through the ADaM-binding site.** A, structure of Lusianthridin. B, AMPK activity of bacterially expressed recombinant  $\alpha 2\beta 1\gamma 1$  in the presence of increasing concentrations of Lusianthridin or Lusianthridin. AMPK activity was determined using the HTRF KinEASE assay kit, and results are presented as fold increase in AMPK activity ( $\pm$ SEM,  $n = 3$ ) relative to the activity in the absence of activator. C and D, pACC HTRF analysis of stable cell lines expressing  $\beta 1$  WT/S108A (C) or  $\beta 2$  WT/S108A (D) treated with Lusianthridin. Results are presented as the fold increase in pACC HTRF signal and are means  $\pm$  SEM of at least three independent experiments. ADaM, allosteric drug and metabolite; AMPK, AMP-activated protein kinase; HTRF, Homogenous Time-Resolved Fluorescence; pACC, phospho-ACC.

regulatory sites in AMPK that direct activators have been shown to bind to (i) the cystathionine  $\beta$ -synthase domains in the  $\gamma$  subunit and (ii) the ADaM site located at the interface between the  $\alpha$  and  $\beta$  subunits. We showed *in vitro* that Lusianthridin activated the AMPK  $\gamma 1$  R299G mutant, which interferes with allosteric activation by AMP (26), but its effects were abolished in various AMPK complexes, including (i) a  $\beta 1$  S108A mutant, (ii) a mutant with a deletion of the CBM of the  $\beta 1$  subunit, and (iii)  $\beta 2$ -containing complexes. The maximal activation of AMPK by Lusianthridin was lower compared with A-769662; however, similar to other ADaM site activators with different stimulatory abilities, the reasons for this difference are not clear based on our currently understanding of the molecular mechanism of ADaM-site activators. Furthermore, the ability of Lusianthridin to protect AMPK from dephosphorylation by PP2C $\alpha$  was altered in the  $\beta 1$  S108A mutant. Lusianthridin-induced phosphorylation of ACC in U2OS cells was profoundly reduced in stable cell lines ( $\beta 1\beta 2$  DKO background) re-expressing a  $\beta 1$  S108A mutant, WT  $\beta 2$ , or  $\beta 2$  S108A mutant compared to  $\beta 1$  WT. Consistent with these observations, we show that activation of AMPK in the  $\beta 1$  KO U2OS cells, thus expressing only  $\beta 2$  complexes, was blunted after Lusianthridin treatment. This activation profile is characteristic of activators at the ADaM-binding site, including activation of AMPK by a benchmark compound A-769662 (31), suggesting that Lusianthridin binds to the same site. The phosphorylated  $\beta 1$  S108 residue within the CBM provides

important interactions with residues in the AMPK $\alpha$  subunit kinase domain, explaining the observations that mutation or truncation of this region affects the action of ADaM site-binding activators. The observation that  $\beta 2$ -containing complexes affect A-769662 and Lusianthridin is not clear from our current structural understanding of this site, primarily because there is no high-resolution cocrystal structure of the  $\beta 2$ -containing AMPK trimeric complex and an ADaM site-binding activator. Furthermore, some potent ADaM-site compounds (e.g., 991) are less impacted by a switch to  $\beta 2$ -containing complexes (27), which may simply reflect the fact that these compounds bind tighter compared with A-769662 and Lusianthridin.

Previous studies have shown that the activity of synthetic ADaM site-binding compounds, such as A-769662, is impaired in  $\beta 1$  S108A mutant and WT  $\beta 2$  complex compared with the  $\beta 1$  WT cell line, although an increase in AMPK activity is observed at higher doses (300  $\mu$ M) (20) (Fig. S10). We observe with our stable cell lines that there is a sharp increase in AMPK activity above 100  $\mu$ M A-769662, which could be due to a perturbation in ATP production (e.g., by cellular toxicity) leading to indirect activation of AMPK and not through the ADaM-binding site (Fig. S10). Therefore, concentration and duration of the compound needs to be carefully assessed, and in general, concentrations >100  $\mu$ M are not recommended to be used in cells when studying the effects of A-769662 through the ADaM-binding site. The authors monitored activation of AMPK after immunoprecipitation of the expressed complexes, which only captures the intrinsic activity of AMPK $\alpha$  (regulated by Thr172 phosphorylation). It has been reported that ADaM site activators are strongly driven by allosteric activation in cells (29, 44, 45), which is not captured by the *in vitro* AMPK activity assay after immunoprecipitation. Therefore, changes in phosphorylation of Thr172 are only observed at higher concentrations of A-769662 than those that cause increases in phosphorylation of ACC. We show in our U2OS WT cells that A-769662 induces phosphorylation of ACC in the region of an EC<sub>50</sub> of 10  $\mu$ M. The advantage of the U2OS stable cell system that we have generated is that these complexes are expressed in the AMPK $\beta 1\beta 2$  DKO background, so phosphorylation of ACC can be used to monitor cellular AMPK activation, which is complicated by the presence of endogenously expressed AMPK in other cell systems that rely on displacement of endogenous cellular  $\beta 1$  subunits (20). Therefore, U2OS cells stably expressing the  $\beta 1$ -WT,  $\beta 1$ -S108A mutant, WT- $\beta 2$ , or  $\beta 2$ -S108A mutant in an AMPK $\beta 1\beta 2$  DKO background will be a more suitable tool in identifying and assessing the activation of AMPK through the ADaM site and  $\beta$ -specific activators.

Similar to A-769662, we observed a sharp increase in phospho-ACC in  $\beta 1$ -KO cells and  $\beta 1$ -/ $\beta 2$ -S108A mutant and  $\beta 2$ -WT stable cell lines at high concentrations of Lusianthridin (above 100  $\mu$ M) (Fig. S10). This likely occurs through a decrease in ATP production and indirect activation of AMPK as revealed through measurement of the adenine nucleotide levels within the cells (Fig. S11). Lusianthridin did not have

## Natural plant compounds directly regulate AMPK

significant effect on oxygen consumption rate up to 100  $\mu\text{M}$  (Fig. S11). This is consistent with a previous report for salicylic acid that at low concentrations, salicylic acid activates AMPK through the ADaM-binding site, and at high concentrations, salicylic acid perturbs the nucleotide status of the cell, and this leads to indirect activation of AMPK in cells (20). In contrast, the majority of natural activators work through an indirect effect, for example, quercetin, which we show here increases phospho-ACC in  $\beta 1$  WT and  $\beta 2$  WT cell lines to a similar extent, consistent with its reported ability to increase ATP levels and indirectly activate AMPK (Fig. S10C). Taken together, these  $\beta 1$ -WT and  $\beta 2$ -WT and S108A stable cells robustly show the contribution of the ADaM site in mediating the activation of AMPK by various compounds. We show that concentrations of Lusianthridin below 100  $\mu\text{M}$  regulate AMPK almost exclusively through its ability to bind to the ADaM-binding site in AMPK.

AMPK plays an important role in maintaining energy homeostasis within the liver by primarily inhibiting lipid and cholesterol synthesis and increasing fatty acid oxidation (6, 46, 47). As a consequence of its beneficial effects on liver lipid homeostasis, AMPK has been implicated in treating metabolic diseases with underlying problems in liver lipid metabolism, including nonalcoholic fatty liver disease. Activation of AMPK has been reported to be beneficial in hepatic lipid metabolism in preclinical models (48). Interestingly, direct activation of the  $\beta 1$ -isoform through the ADaM site was demonstrated to improve nonalcoholic fatty liver disease (49), suggesting that ADaM-site activators, which are often more  $\beta 1$  selective, are likely to be effective in treating fatty liver diseases. In line with this, we have demonstrated that Lusianthridin dose-dependently activates AMPK, which is associated with a corresponding decrease in *de novo* lipogenesis in mouse primary hepatocytes. We show that the Lusianthridin effect (when treated up to 40  $\mu\text{M}$ ) was lost in hepatocytes taken from mice with a DKI mutation in ACC1/2 at the AMPK-phosphorylation site (43), demonstrating that Lusianthridin-induced inhibition of lipogenesis is mediated by its ability to activate AMPK. Consistent with this, Lusianthridin, but not AICAR, displayed blunted increases in ACC phosphorylation, which was associated with an attenuated inhibition of lipogenesis in the  $\beta 1$  S108A compared with the WT hepatocytes. These results provide genetic evidence that Lusianthridin inhibits *de novo* lipogenesis in an AMPK-dependent manner by binding to the ADaM site (under a certain range of concentrations) and through phosphorylation of ACC, which is similar to the action of salicylic acid (20, 50).

The discovery that Lusianthridin directly activates AMPK prompted us to study previous literature published on this compound. Members of the dihydrophenanthrene series have been reported as plant phytoalexins that are produced in response to a pathogen infection (51). Previous studies have reported that Lusianthridin elicits an antimigratory effect (52) (0.5  $\mu\text{M}$ , >12 h) and has anticancer properties (10–20  $\mu\text{M}$ , >72 h) (53). It would be interesting to determine whether the ability of Lusianthridin to elicit these effects is

mediated through regulation of AMPK using genetic KO models. Dihydrophenanthrene natural products have been reported in a number of families, including the Orchidaceae (54), Dioscoreaceae (55), and Cannabinaceae (56). Interestingly, these families also accumulate a number of related compounds belonging both to the dihydrophenanthrene (to which Lusianthridin belongs) and the phenanthrene (to which Lusianthrin belongs) groups. The distribution and biological activities of phenanthrenes has been recently reviewed (57). This added to the present demonstration that the natural phenanthrene Lusianthrin directly activated AMPK through a mechanism similar to Lusianthridin and incited us to investigate in more detail the structure–activity relationship toward AMPK activation that could occur in these groups of natural products.

The identification of natural plant dihydrophenanthrenes and phenanthrenes that directly activate AMPK through the ADaM site is an intriguing finding and builds on the previous discovery that another natural product, salicylic acid, also directly activates AMPK at this novel regulatory site. This raises the distinct possibility that other natural plant compounds may share the same common mechanism of action. Alternatively, it may be completely coincidental that these compounds contain the correct chemical properties to bind at the ADaM site, albeit at a lower affinity compared with synthetic direct activators like A-769662 and 991. It is also entirely possible that a more potent natural plant AMPK activator(s) already exists. An intriguing possibility is that these natural compounds may directly activate AMPK found in plants (sucrose nonfermenting-related kinase [SnRK]), although very little is understood about the SnRK proteins and regulation by small molecules. It could be advantageous for plants to be able to modulate its energy homeostasis in response to an infection, and activation of AMPK may represent a mechanism to do this. It will be interesting to understand whether endogenous ligands in plants play a role in directly regulating SnRK.

Natural plant compounds that have been shown to activate AMPK are often produced in response to infection, and because of their likely toxic nature, it was previously assumed that all natural plant compounds indirectly activate AMPK because of inhibition of ATP production. Often natural compounds have been overlooked as potentially important activators of AMPK because of this conjecture. Our study provides further evidence that some natural plant compounds directly activate AMPK, and further natural compounds are likely to be discovered that also activate AMPK through the ADaM site. Our current study mainly focuses on the kinetics and mechanism of action in an *in vitro* setting. For any future application(s), robust studies are required to assess (dihydro)phenanthrenes *in vivo* particularly paying close attention to the safety profile of these ingredients and their bioavailability. Finally, when the ADaM site was discovered, it was proposed that a natural endogenous mammalian metabolite may bind at this site and regulate AMPK. A recent study with endogenous long-chain fatty acyl-CoAs (36) and our study provide growing support that

natural compounds may bind to this novel regulatory site on AMPK. It is an exciting time in the AMPK field as work continues to assess whether the ADaM site has a major physiological role to play in mammals.

## Experimental procedures

### Materials

A number of compounds were used in this study, AICAR (Apollo Scientific; catalog no.: OR1170T), 991 (5-[[6-chloro-5-(1-methylindol-5-yl)-1H-benzimidazol-2-yl]oxy]-2-methylbenzoic acid; CAS number: 129739-36-2) (44), and A-769662 (Selleckchem; catalog no.: S2697). STO-609 was purchased from Tocris. Ionomycin was from MilliporeSigma. Cell culture media were purchased from Invitrogen. All other reagents were from MilliporeSigma if not otherwise stated.

### Source and quality control of Lusianthridin

Lusianthridin (CAS: 87530-30-1) was purchased from Analyticon (catalog no.: NP-012362) or custom synthesized by Syngene. Quality control of Lusianthridin samples from the initial screening library compared with the one obtained by synthesis is shown in Fig. S1. We proceeded with caution when sourcing Lusianthridin for our studies since we received compounds from some suppliers that had the same molecular weight but the incorrect MS/MS pattern, confirming that the identity was not Lusianthridin (data not shown).

### Antibodies

ACC (catalog no.: 3676), phospho-ACC1 (Ser79; catalog no.: 3661), AMPK $\alpha$  (catalog no.: 2532), phospho-AMPK $\alpha$  (Thr172; catalog no.: 2535), AMPK $\beta$ 1 (catalog no.: 4178), Raptor (catalog no.: 2280), phospho-Raptor (S792; catalog no.: 2083), AMPK $\beta$ 1 (catalog no.: 12063), AMPK $\beta$ 2 (catalog no.: 4148), and AMPK $\beta$ 1/2 (catalog no.: 4150) were obtained from Cell Signaling Technology. Antibody against AMPK $\gamma$ 1 (catalog no.: ab32508) was purchased from Abcam, and tubulin (catalog no.: T6074), FLAG (catalog no.: F7425), and  $\beta$ -actin (catalog no.: A2228) were purchased from MilliporeSigma. HTRF assay for detection of phospho-ACC was obtained from Cisbio (catalog no.: 64ACCPET).

### Animal ethics and models

All the animal experiments were performed accordingly with the European guidelines approved by the Switzerland authorization to experiment on vertebrates under license VD3247 and the approval from internal ethics committee at Nestle Research (ASP-17-03-INT) or were in accordance with McMaster Animal Care Committee guidelines (AUP: 16-12-41, Hamilton, ON). Generation of the ACC1/2 phospho-deficient KI mice, ACC1 (Ser79Ala)/ACC2(Ser212Ala), and AMPK $\beta$ 1 Ser108Ala KI mice were previously described (43, 58).

### Plasmids

All plasmid constructs were generated using standard molecular biology techniques. Construction of the polycistronic

AMPK expression vector for bacterial expression (59) containing N-terminally His-tagged human AMPK $\alpha$ 2 (NM\_006252), AMPK $\beta$ 1 (NM\_006253), and AMPK $\gamma$ 1 (NM\_002733) has been previously described (47). For expression of the AMPK subunits in mammalian cells (stable cell lines), human FLAG- $\beta$ 1 or FLAG- $\beta$ 2 was cloned into a pcDNA5-FRT vector under the cytomegalovirus promoter. Site-directed mutagenesis was carried out according to the QuikChange method (Stratagene) using KOD polymerase (Novagen). Sequences were verified utilizing the BigDyeR Terminator 3.1 kit on a 3500XL Genetic analyzer (ABI-Invitrogen).

### Bacterial protein expression and purification

Recombinant N-terminally His-tagged AMPK complexes were expressed in *Escherichia coli* and purified using nickel affinity chromatography and gel filtration as described previously (27). AMPK was phosphorylated on  $\alpha$ Thr172 by overnight incubation with Mg.ATP and recombinant CaMKK2 and further purified with a final gel filtration step (27). A stock solution of the activated AMPK complex was prepared at around 5 mg/ml in 50 mM Tris (pH 8.0), 300 mM NaCl, and 1 mM Tris(2-carboxyethyl)phosphine.

### AMPK assay and high-throughput screen

An HTRF-based assay was adopted for the high-throughput screen to measure the activity of AMPK in response to test samples (KinEASE STK S1 kit; Cisbio). We have previously published this method (37), but briefly, the screen was carried out in a 384-well format, with approximately 26 ng/ml purified AMPK enzyme (human AMPK $\alpha$ 2 $\beta$ 1 $\gamma$ 1 complex), ATP (100  $\mu$ M), and a generic biotinylated Ser/Thr protein kinase substrate (STK1; Cisbio). The enzymatic reaction was carried out for 30 min at 30 °C in the absence or the presence of test samples including crude extracts and complex fractions (100  $\mu$ g/ml) or pure compounds and semipure fractions (10  $\mu$ M) in 1% dimethyl sulfoxide final concentration.

The amount of phosphorylated substrate was determined by adding an antiphospho-STK-S1 antibody (Cisbio) coupled to europium cryptate (donor) and a streptavidin coupled to XL665 (acceptor), which binds the biotinylated substrate. Upon excitation at 330 nm, the europium cryptate emits light at 620 nm. If the donor and acceptor come in close proximity, FRET occurs, leading to signal emission at 665 nm from the acceptor. This signal is proportional to the amount of phosphorylated substrate. The ratio between 665/620 was measured using a Synergy Neo multimode reader (BioTek) and correlates to AMPK activity.

### In vitro protein kinase screen

All protein kinases in the kinase panel were expressed, purified, and assayed at the International Centre for Protein Kinase Profiling (<http://www.kinase-screen.mrc.ac.uk/>), MRC Protein Phosphorylation and Ubiquitylation Unit, University of Dundee, as previously described (40). The compound was screened in duplicate and the data reported as the percentage

## Natural plant compounds directly regulate AMPK

of activity when compared with a control without compound,  $\pm$  SD).

### HTRF cell-free assay

Phosphorylated recombinant AMPK was incubated with varying concentrations of ligand for 30 min using substrate and reagents from the HTRF-KinEASE Cisbio assay kit (STK S1 Kit). Phosphorylation of the substrate was measured after 2 h at room temperature as per the manufacturer's protocol (37), and phosphorylated peptide was detected by performing HTRF. The 665 nm/620 nm ratio was determined, and the results are plotted as fold activation compared with the respective AMPK complex without any compound.

### AMPK protection against dephosphorylation assay

The assay was performed as previously described (26). Briefly, the purified and phosphorylated (as described previously) human AMPK (either  $\alpha 2\beta 1\gamma 1$  or  $\alpha 2\beta 1\gamma 1$  S108A) was incubated for 10 min at 37 °C with recombinant PP2C $\alpha$ , in the presence or the absence 5 mM MgCl<sub>2</sub>, along with either AMP, A-769662, or Lusianthridin as indicated in the figure legend. Reactions were terminated by the addition of SDS-gel loading buffer, and AMPK $\alpha$  T172 phosphorylation was determined by Western blotting.

### Cell culture

U2OS Flp-In T-Rex cells were a kind gift from John Rouse (MRC Protein Phosphorylation and Ubiquitylation Unit, University of Dundee). Cells were cultured in Dulbecco's modified Eagle's medium (DMEM)–Glutamax supplemented with 10% fetal calf serum and 1% penicillin–streptomycin. Cells were seeded and incubated at 37 °C overnight before use in experiments. For Western blot analysis, cells were washed with PBS and scraped into lysis buffer (50 mM Hepes, 150 mM NaCl, 100 mM NaF, 10 mM sodium pyrophosphate, 5 mM EDTA, 250 mM sucrose, 1 mM DTT, 1% Triton X-100, 1 mM sodium orthovanadate, 0.5 mM PMSF, 1 mM benzamide HCl, 1  $\mu$ g/ml leupeptin, 1  $\mu$ g/ml pepstatin A, and 1 mM microcystin-LR). Lysates were centrifuged at 21,300g for 15 min, and protein concentration from the supernatant was determined using Bradford reagent (Thermo Fisher Scientific) and bovine serum albumin as standard.

### Phospho-ACC HTRF Cisbio assay

Unless otherwise specified, cells were seeded at 50,000 cells per well in a 96-well plate and treated the following day with the indicated treatments as described in the figures, in cell culture media lacking fetal bovine serum. Cells were lysed by adding 50  $\mu$ l of the Cisbio lysis buffer for 30 min at room temperature before 16  $\mu$ l of lysate was incubated with 4  $\mu$ l of the two antibodies in the phospho-ACC HTRF kit (1:40 dilution) as per the manufacturer's protocol. Cell lysates were incubated overnight before the ratio of 665/620 nm was determined using a SpectraMax i3 plate reader fitted with a HTRF cartridge (Molecular Devices). For Western blot

analysis, 16  $\mu$ l of lysate was resolved by SDS-PAGE before being subjected to Western blot analysis using the indicated antibodies in the figure legends.

### Western blot analysis

About 20  $\mu$ g of total protein was resolved by SDS-PAGE on 4 to 12% NuPAGE and transferred to Odyssey nitrocellulose membranes (LI-COR Biosciences). Membranes were blocked for 1 h at room temperature in LI-COR blocking buffer (catalog no.: 927-60001; LI-COR Biosciences). The membranes were subsequently incubated with primary antibodies (1:1000 dilution) in 10 mM Tris (pH 7.6), 137 mM NaCl, and 0.1% (v/v) Tween-20 containing 5% (w/v) bovine serum albumin overnight at 4 °C. Primary antibodies were detected using LI-COR IRDye infrared dye secondary antibodies (1:10,000 dilution) and visualized using an Odyssey Infrared imager (LI-COR Biosciences). Quantification of the bands was performed using the Odyssey software and expressed as a ratio of the signal obtained with the phospho-specific antibody relative to the appropriate total antibody. For capillary Western blotting, cell lysates were diluted in Sally Sue SDS buffer to 0.2 mg/ml (60). Samples were prepared and analyzed according to the manufacturer's instructions (ProteinSimple).

### CRISPR/Cas9-mediated deletion of AMPK $\beta$

AMPK $\beta 1$  single and AMPK $\beta 1/\beta 2$  DKO U2OS Flp-In T-Rex cell lines were generated by Horizon Discovery. For the AMPK $\beta 1$  single KO cells, plasmids contain Cas9 and guide sequence targeting the first exon of AMPK $\beta 1$  (GAAG ACGCCGACCTCTTCCA). Once a homozygous AMPK $\beta 1$  KO clone was identified, the AMPK $\beta 1/\beta 2$  DKO was generated with plasmid containing Cas9 and guide sequence targeting the first exon of AMPK $\beta 2$  (CCCGGCCCACTGTTATCCGC). Cells were genotyped and analyzed by Western blotting to determine AMPK $\beta 1$  and AMPK $\beta 1/\beta 2$  expression.

### Generation of isogenic stable cell lines

Stable cell lines expressing human  $\beta 1/2$  (WT or S108A mutant) under a constitutive promoter were made using the Flp-In system (Invitrogen), in the U2OS Flp-In T-Rex AMPK $\beta 1/\beta 2$  DKO background. The AMPK  $\beta$  subunits were cloned into an Flp-In expression vector and cotransfected with the Flp recombinase vector, pOG44, which results in targeted integration of the expression vector to the same locus in every cell (integrated FRT site) ensuring homogeneous high levels of gene expression. U2OS Flp-In T-Rex AMPK $\beta 1/\beta 2$  DKO cells ( $1 \times 10^6$ ) were plated in a 10 cm dish in medium containing selection antibiotics. On the day of transfection, cells were washed once with PBS, and fresh medium was added without additional antibiotics. Complementary DNA constructs encoding FLAG-AMPK  $\beta 1/2$  WT or  $\beta 1/2$  S108A mutant were transfected along with pOG44 (1:9) using FUGENE HD transfection reagent (Promega; catalog no.: E2311). About 24 h post transfection, medium was replaced with fresh medium

without additional antibiotics. About 48 h post transfection, cells were trypsinized and divided into two 20 cm culture dishes containing fresh medium. About 24 h later, cells were cultured in medium containing 200 µg/ml hygromycin B (Thermo Fisher Scientific; catalog no.: 10687010). Medium was replaced every 2 to 3 days until resistant colonies appeared. Single colonies were isolated using cloning rings (MilliporeSigma; catalog no.: C1059) and expanded and maintained in selection medium containing 200 µg/ml hygromycin B.

### Hepatocyte isolation and lipogenesis assay

Primary hepatocytes were isolated from the indicated mice (10–15 week old males) by collagenase perfusion and cultured as previously described (43, 61). Briefly, the cells were plated in M199 medium containing Glutamax and supplemented with 100 U/ml penicillin, 100 µg/ml streptomycin, 10% (v/v) fetal calf serum, 500 nM dexamethasone (MilliporeSigma), 100 nM triiodothyronine (MilliporeSigma), and 10 nM insulin (MilliporeSigma). The hepatocytes were attached for 4 h and then maintained in M199 medium with antibiotics and 100 nM dexamethasone for 16 h. The experiments were performed the following morning by treating with the compounds (as indicated in the figure legends) followed by cell lysis for Western blot analysis or lipogenesis assay. Rate of *de novo* lipogenesis in mouse primary hepatocytes was measured as incorporation of [<sup>14</sup>C] into fatty acids using [1-<sup>14</sup>C]-acetate (PerkinElmer) as substrate (43, 47).

### Oxygen consumption measurements

Oxygen consumption in isolated HepG2 cells was measured in a Seahorse XFe96 instrument (Agilent Seahorse). HepG2 cells were seeded directly into Seahorse 96-well tissue culture plates (XFe96 FluxPak; catalog no.: 102416-100; Agilent) at a density of 20,000 cells per well. Two days after seeding, the cells were washed twice in DMEM (XF DMEM, pH 7.4; catalog no.: 103575-100; Agilent) with 5 mM glucose, 2 mM glutamine, 1 mM sodium pyruvate added. The cells were allowed to equilibrate for 20 min and maintained at 37 °C during the experiment. Respiration rates were determined every 6 min before and after stimulation with compounds. Respiratory chain inhibitors were added at the following final concentrations: complex V inhibitor oligomycin (2.5 µg/ml), complex I inhibitor rotenone (1 µM), complex III inhibitor antimycin A (1 µg/ml), and the protonophore FCCP (2 µM).

### Nucleotide measurements

Treated cells were extracted with ice-cold extraction solution MeOH:H<sub>2</sub>O:CHCl<sub>3</sub> (methanol:water:chloroform) in a proportion of 5:3:5 containing <sup>13</sup>C standards. The resulting upper phase was recovered and dried overnight in a vacuum centrifuge (Labconco). Prior to measurement, dried samples were dissolved in 60% (v/v) acetonitrile/H<sub>2</sub>O, and supernatants were analyzed by LC-MS.

Metabolites were separated on ZIC-philic column (100 × 2.1 mm, 5 µm, Merck Sequant) with solvent A being H<sub>2</sub>O

containing 10 mM ammonium acetate (NH<sub>4</sub>Ac) and 0.04% (v/v) ammonium hydroxide (NH<sub>4</sub>OH), pH ~9.3 and solvent B being acetonitrile. A linear gradient from 90% to 25% B was applied, and eluting metabolites were analyzed with an Orbitrap Fusion Lumos mass spectrometer (Thermo Fisher Scientific) with spray voltages of 3500 and 3000 V for positive and negative mode, respectively. The full scan was measured with on-the-fly alternating positive and negative mode scans, which covered *m/z* ranges from 75 to 750 and from 85 to 850, respectively, at a resolution of 60,000. Instrument control and data analysis was conducted using Xcalibur (Thermo Fisher Scientific).

### Data availability

All the data are contained within the article.

*Supporting information*—This article contains supporting information.

*Acknowledgments*—We acknowledge the contribution of Eva Martin, Mayuko Tamura, Carles Canto, and Jose-Luis Sanchez Garcia throughout the study. The authors acknowledge the provision of ACC DKI mice to G. R. S. from Prof. Bruce Kemp, St. Vincent's Institute of Medical Research, Australia. Nordisk Foundation Center for Basic Metabolic Research is an independent research center based at the University of Copenhagen, Denmark and partially funded by an unconditional donation from the Novo Nordisk Foundation (grant number: NNF18CC0034900).

*Author contributions*—M. J. S., K. S., and D. B. conceptualization; M. J. S., Y. R., K. N., N. B., E. A. D., O. C., M. N. P., M. D., and B. B. methodology; M. J. S., Y. R., K. N., N. B., E. A. D., O. C., M. N. P., M. D., and B. B. formal analysis; M. J. S., Y. R., K. N., N. B., E. A. D., O. C., M. N. P., M. D., and B. B. investigation; G. R. S. data curation; M. J. S., Y. R., K. N., N. B., E. A. D., O. C., S. L., M. N. P., M. D., B. B., S. C., G. R. S., D. B., and K. S. writing—reviewing & editing.

*Funding and additional information*—G. R. S. is supported by a Diabetes Canada Investigator Award (grant no.: DI-5-17-5302-GS), a Canadian Institutes of Health Research Foundation Grant (grant no.: 201709FDN-CEBA-116200), a Tier 1 Canada Research Chair and a J. Bruce Duncan Endowed Chair in Metabolic Diseases. K. S. is supported by a project grant from the Novo Nordisk Foundation (grant no.: NNF21OC0070257). The authors acknowledge the provision of ACC DKI mice to G.R.S. from Prof. Bruce Kemp, St. Vincent's Institute of Medical Research, Australia.

*Conflict of interest*—M. J. S., Y. R., K. N., O. C., M. N. P., B. B., and D. B. are current and K. S., N. B., and M. D. were former employees of Nestlé Research (Switzerland). McMaster University has received funding from Nestlé Research (Switzerland) for research in the laboratory of G. R. S. All other authors declare that they have no conflicts of interest with the contents of this article.

*Abbreviations*—The abbreviations used are: ADaM, allosteric drug and metabolite; AICAR, 5-aminoimidazole-4-carboxamide riboside; AMPK, AMP-activated protein kinase; CaMKK2, calcium/calmodulin-dependent protein kinase 2; CAS, Chemical Abstracts Service; CBM, carbohydrate-binding module; DKI, double knock-in; DKO, double knock-out; DMEM, Dulbecco's modified Eagle's

## Natural plant compounds directly regulate AMPK

medium; HTRF, Homogenous Time-Resolved Fluorescence; KI, knock-in; KO, knock-out; PP2C $\alpha$ , protein phosphatase 2C $\alpha$ ; SnRK, sucrose nonfermenting-related kinase.

### References

1. Rena, G., and Sakamoto, K. (2014) Salicylic acid: Old and new implications for the treatment of type 2 diabetes? *Diabetol. Int.* **5**, 212–218
2. Katsyuba, E., Romani, M., Hofer, D., and Auwerx, J. (2020) NAD(+) homeostasis in health and disease. *Nat. Metab.* **2**, 9–31
3. Bailey, C. J. (2017) Metformin: Historical overview. *Diabetologia* **60**, 1566–1576
4. Leri, M., Scuto, M., Ontario, M. L., Calabrese, V., Calabrese, E. J., Buciantini, M., and Stefani, M. (2020) Healthy effects of plant polyphenols: Molecular mechanisms. *Int. J. Mol. Sci.* **21**, 1250
5. Grahame Hardie, D. (2016) Regulation of AMP-activated protein kinase by natural and synthetic activators. *Acta Pharm. Sin B* **6**, 1–19
6. Steinberg, G. R., and Carling, D. (2019) AMP-activated protein kinase: The current landscape for drug development. *Nat. Rev. Drug Discov.* **18**, 527–551
7. Hardie, D. G. (2011) AMP-activated protein kinase: An energy sensor that regulates all aspects of cell function. *Genes Dev.* **25**, 1895–1908
8. Herzig, S., and Shaw, R. J. (2018) Ampk: Guardian of metabolism and mitochondrial homeostasis. *Nat. Rev. Mol. Cell Biol.* **19**, 121–135
9. Hawley, S. A., Davison, M., Woods, A., Davies, S. P., Beri, R. K., Carling, D., and Hardie, D. G. (1996) Characterization of the AMP-activated protein kinase from rat liver and identification of threonine 172 as the major site at which it phosphorylates AMP-activated protein kinase. *J. Biol. Chem.* **271**, 27879–27887
10. Xiao, B., Sanders, M. J., Underwood, E., Heath, R., Mayer, F. V., Carmena, D., Jing, C., Walker, P. A., Eccleston, J. F., Haire, L. F., Saiu, P., Howell, S. A., Aasland, R., Martin, S. R., Carling, D., et al. (2011) Structure of mammalian AMPK and its regulation by ADP. *Nature* **472**, 230–233
11. Oakhill, J. S., Steel, R., Chen, Z. P., Scott, J. W., Ling, N., Tam, S., and Kemp, B. E. (2011) AMPK is a direct adenylate charge-regulated protein kinase. *Science* **332**, 1433–1435
12. Gowans, G. J., Hawley, S. A., Ross, F. A., and Hardie, D. G. (2013) AMP is a true physiological regulator of AMP-activated protein kinase by both allosteric activation and enhancing net phosphorylation. *Cell Metab.* **18**, 556–566
13. Hawley, S. A., Ross, F. A., Chevtzoff, C., Green, K. A., Evans, A., Fogarty, S., Towler, M. C., Brown, L. J., Ogunbayo, O. A., Evans, A. M., and Hardie, D. G. (2010) Use of cells expressing gamma subunit variants to identify diverse mechanisms of AMPK activation. *Cell Metab.* **11**, 554–565
14. Hawley, S. A., Ford, R. J., Smith, B. K., Gowans, G. J., Mancini, S. J., Pitt, R. D., Day, E. A., Salt, I. P., Steinberg, G. R., and Hardie, D. G. (2016) The Na<sup>+</sup>/Glucose cotransporter inhibitor canagliflozin activates AMPK by inhibiting mitochondrial function and increasing cellular AMP levels. *Diabetes* **65**, 2784–2794
15. Jenkins, Y., Sun, T. Q., Markovtsov, V., Foretz, M., Li, W., Nguyen, H., Li, Y., Pan, A., Uy, G., Gross, L., Baltgalvis, K., Yung, S. L., Gururaja, T., Kinoshita, T., Owyang, A., et al. (2013) AMPK activation through mitochondrial regulation results in increased substrate oxidation and improved metabolic parameters in models of diabetes. *PLoS One* **8**, e81870
16. Marcinko, K., Bujak, A. L., Lally, J. S., Ford, R. J., Wong, T. H., Smith, B. K., Kemp, B. E., Jenkins, Y., Li, W., Kinsella, T. M., Hitoshi, Y., and Steinberg, G. R. (2015) The AMPK activator R419 improves exercise capacity and skeletal muscle insulin sensitivity in obese mice. *Mol. Metab.* **4**, 643–651
17. LaMoia, T. E., and Shulman, G. I. (2021) Cellular and molecular mechanisms of metformin action. *Endocr. Rev.* **42**, 77–96
18. Hunter, R. W., Hughey, C. C., Lantier, L., Sundelin, E. I., Peggie, M., Zeqiraj, E., Sicheri, F., Jessen, N., Wasserman, D. H., and Sakamoto, K. (2018) Metformin reduces liver glucose production by inhibition of fructose-1-6-bisphosphatase. *Nat. Med.* **24**, 1395–1406
19. Foretz, M., Hebrard, S., Leclerc, J., Zarrinpashneh, E., Soty, M., Mithieux, G., Sakamoto, K., Andreelli, F., and Viollet, B. (2010) Metformin inhibits hepatic gluconeogenesis in mice independently of the LKB1/AMPK pathway via a decrease in hepatic energy state. *J. Clin. Invest.* **120**, 2355–2369
20. Hawley, S. A., Fullerton, M. D., Ross, F. A., Schertzer, J. D., Chevtzoff, C., Walker, K. J., Peggie, M. W., Zibrova, D., Green, K. A., Mustard, K. J., Kemp, B. E., Sakamoto, K., Steinberg, G. R., and Hardie, D. G. (2012) The ancient drug salicylate directly activates AMP-activated protein kinase. *Science* **336**, 918–922
21. Din, F. V., Valanciute, A., Houde, V. P., Zibrova, D., Green, K. A., Sakamoto, K., Alessi, D. R., and Dunlop, M. G. (2012) Aspirin inhibits mTOR signaling, activates AMP-activated protein kinase, and induces autophagy in colorectal cancer cells. *Gastroenterology* **142**, 1504–1515.e3
22. Steinberg, G. R., Dandapani, M., and Hardie, D. G. (2013) Ampk: Mediating the metabolic effects of salicylate-based drugs? *Trends Endocrinol. Metab.* **24**, 481–487
23. Smith, B. K., Ford, R. J., Desjardins, E. M., Green, A. E., Hughes, M. C., Houde, V. P., Day, E. A., Marcinko, K., Crane, J. D., Mottillo, E. P., Perry, C. G., Kemp, B. E., Tarnopolsky, M. A., and Steinberg, G. R. (2016) Salsalate (salicylate) uncouples mitochondria, improves glucose homeostasis, and reduces liver lipids independent of AMPK-beta1. *Diabetes* **65**, 3352–3361
24. Goldfine, A. B., Fonseca, V., Jablonski, K. A., Chen, Y. D., Tipton, L., Staten, M. A., Shoelson, S. E., and Targeting Inflammation Using Salsalate in Type 2 Diabetes Study, T (2013) Salicylate (salsalate) in patients with type 2 diabetes: A randomized trial. *Ann. Intern. Med.* **159**, 1–12
25. Salastekar, N., Desai, T., Hauser, T., Schaefer, E. J., Fowler, K., Joseph, S., Shoelson, S. E., Goldfine, A. B., and team, T.-C. s. (2017) Salsalate improves glycaemia in overweight persons with diabetes risk factors of stable statin-treated cardiovascular disease: A 30-month randomized placebo-controlled trial. *Diabetes Obes. Metab.* **19**, 1458–1462
26. Sanders, M. J., Ali, Z. S., Hegarty, B. D., Heath, R., Snowden, M. A., and Carling, D. (2007) Defining the mechanism of activation of AMP-activated protein kinase by the small molecule A-769662, a member of the thienopyridone family. *J. Biol. Chem.* **282**, 32539–32548
27. Xiao, B., Sanders, M. J., Carmena, D., Bright, N. J., Haire, L. F., Underwood, E., Patel, B. R., Heath, R. B., Walker, P. A., Hallen, S., Giordanetto, F., Martin, S. R., Carling, D., and Gamblin, S. J. (2013) Structural basis of AMPK regulation by small molecule activators. *Nat. Commun.* **4**, 3017
28. Cool, B., Zinker, B., Chiou, W., Kifle, L., Cao, N., Perham, M., Dickinson, R., Adler, A., Gagne, G., Iyengar, R., Zhao, G., Marsh, K., Kym, P., Jung, P., Camp, H. S., et al. (2006) Identification and characterization of a small molecule AMPK activator that treats key components of type 2 diabetes and the metabolic syndrome. *Cell Metab.* **3**, 403–416
29. Goransson, O., McBride, A., Hawley, S. A., Ross, F. A., Shpiro, N., Foretz, M., Viollet, B., Hardie, D. G., and Sakamoto, K. (2007) Mechanism of action of A-769662, a valuable tool for activation of AMP-activated protein kinase. *J. Biol. Chem.* **282**, 32549–32560
30. Scott, J. W., van Denderen, B. J., Jorgensen, S. B., Honeyman, J. E., Steinberg, G. R., Oakhill, J. S., Iseli, T. J., Koay, A., Gooley, P. R., Stapleton, D., and Kemp, B. E. (2008) Thienopyridone drugs are selective activators of AMP-activated protein kinase beta1-containing complexes. *Chem. Biol.* **15**, 1220–1230
31. Calabrese, M. F., Rajamohan, F., Harris, M. S., Caspers, N. L., Magyar, R., Withka, J. M., Wang, H., Borzilleri, K. A., Sahasrabudhe, P. V., Hoth, L. R., Geoghegan, K. F., Han, S., Brown, J., Subashi, T. A., Reyes, A. R., et al. (2014) Structural basis for AMPK activation: Natural and synthetic ligands regulate kinase activity from opposite poles by different molecular mechanisms. *Structure* **22**, 1161–1172
32. Cameron, K. O., and Kurumbail, R. G. (2016) Recent progress in the identification of adenosine monophosphate-activated protein kinase (AMPK) activators. *Bioorg. Med. Chem. Lett.* **26**, 5139–5148
33. Myers, R. W., Guan, H. P., Ehrhart, J., Petrov, A., Prahallada, S., Tozzo, E., Yang, X., Kurtz, M. M., Trujillo, M., Gonzalez Trotter, D., Feng, D., Xu, S., Eiermann, G., Holahan, M. A., Rubins, D., et al. (2017) Systemic pan-AMPK activator MK-8722 improves glucose homeostasis but induces cardiac hypertrophy. *Science* **357**, 507–511

34. Cokorinos, E. C., Delmore, J., Reyes, A. R., Albuquerque, B., Kjobsted, R., Jorgensen, N. O., Tran, J. L., Jatkar, A., Cialdea, K., Esquejo, R. M., Meissen, J., Calabrese, M. F., Cordes, J., Moccia, R., Tess, D., *et al.* (2017) Activation of skeletal muscle AMPK promotes glucose disposal and glucose lowering in non-human primates and mice. *Cell Metab.* **25**, 1147–1159.e10
35. Gluais-Dagorn, P., Foretz, M., Steinberg, G. R., Batchuluun, B., Zawistowska-Deniziak, A., Lambooi, J. M., Guigas, B., Carling, D., Monternier, P. A., Moller, D. E., Bolze, S., and Hallakou-Bozec, S. (2021) Direct AMPK activation corrects NASH in rodents through metabolic effects and direct action on inflammation and fibrogenesis. *Hepatol. Commun.* **6**, 101–119
36. Pinkosky, S. L., Scott, J. W., Desjardins, E. M., Smith, B. K., Day, E. A., Ford, R. J., Langendorf, C. G., Ling, N. X. Y., Nero, T. L., Loh, K., Galic, S., Hoque, A., Smiles, W. J., Ngoei, K. R. W., Parker, M. W., *et al.* (2020) Long-chain fatty acyl-CoA esters regulate metabolism via allosteric control of AMPK beta1 isoforms. *Nat. Metab.* **2**, 873–881
37. Coulerie, P., Ratinaud, Y., Moco, S., Merminod, L., Naranjo Pinta, M., Bocard, J., Bultot, L., Deak, M., Sakamoto, K., Queiroz, E. F., Wolfender, J. L., and Barron, D. (2016) Standardized LCxLC-ELSD fractionation procedure for the identification of minor bioactives via the enzymatic screening of natural extracts. *J. Nat. Prod.* **79**, 2856–2864
38. Ngoei, K. R. W., Langendorf, C. G., Ling, N. X. Y., Hoque, A., Varghese, S., Camerino, M. A., Walker, S. R., Bozikis, Y. E., Dite, T. A., Ovens, A. J., Smiles, W. J., Jacobs, R., Huang, H., Parker, M. W., Scott, J. W., *et al.* (2018) Structural determinants for small-molecule activation of skeletal muscle AMPK alpha2beta2gamma1 by the glucose importagoc SC4. *Cell Chem. Biol.* **25**, 728–737.e9
39. Rajamohan, F., Reyes, A. R., Frisbie, R. K., Hoth, L. R., Sahasrabudhe, P., Magyar, R., Landro, J. A., Withka, J. M., Caspers, N. L., Calabrese, M. F., Ward, J., and Kurumbail, R. G. (2016) Probing the enzyme kinetics, allosteric modulation and activation of alpha1- and alpha2-subunit-containing AMP-activated protein kinase (AMPK) heterotrimeric complexes by pharmacological and physiological activators. *Biochem. J.* **473**, 581–592
40. Bain, J., Plater, L., Elliott, M., Shpiro, N., Hastie, C. J., McLauchlan, H., Klevernic, I., Arthur, J. S., Alessi, D. R., and Cohen, P. (2007) The selectivity of protein kinase inhibitors: A further update. *Biochem. J.* **408**, 297–315
41. Woods, A., Dickerson, K., Heath, R., Hong, S. P., Momcilovic, M., Johnstone, S. R., Carlson, M., and Carling, D. (2005) Ca<sup>2+</sup>/calmodulin-dependent protein kinase-beta acts upstream of AMP-activated protein kinase in mammalian cells. *Cell Metab.* **2**, 21–33
42. Hawley, S. A., Pan, D. A., Mustard, K. J., Ross, L., Bain, J., Edelman, A. M., Frenguelli, B. G., and Hardie, D. G. (2005) Calmodulin-dependent protein kinase kinase-beta is an alternative upstream kinase for AMP-activated protein kinase. *Cell Metab.* **2**, 9–19
43. Fullerton, M. D., Galic, S., Marcinko, K., Sikkema, S., Pulinilkunnil, T., Chen, Z. P., O'Neill, H. M., Ford, R. J., Palanivel, R., O'Brien, M., Hardie, D. G., Macaulay, S. L., Schertzer, J. D., Dyck, J. R., van Denderen, B. J., *et al.* (2013) Single phosphorylation sites in Acc1 and Acc2 regulate lipid homeostasis and the insulin-sensitizing effects of metformin. *Nat. Med.* **19**, 1649–1654
44. Bultot, L., Jensen, T. E., Lai, Y. C., Madsen, A. L., Collodet, C., Kviklyte, S., Deak, M., Yavari, A., Foretz, M., Ghaffari, S., Bellahcene, M., Ashrafian, H., Rider, M. H., Richter, E. A., and Sakamoto, K. (2016) Benzimidazole derivative small-molecule 991 enhances AMPK activity and glucose uptake induced by AICAR or contraction in skeletal muscle. *Am. J. Physiol. Endocrinol. Metab.* **311**, E706–E719
45. Willows, R., Navaratnam, N., Lima, A., Read, J., and Carling, D. (2017) Effect of different gamma-subunit isoforms on the regulation of AMPK. *Biochem. J.* **474**, 1741–1754
46. Boudaba, N., Marion, A., Huet, C., Pierre, R., Viollet, B., and Foretz, M. (2018) AMPK Re-activation suppresses hepatic steatosis but its down-regulation does not promote fatty liver development. *EBioMedicine* **28**, 194–209
47. Hunter, R. W., Foretz, M., Bultot, L., Fullerton, M. D., Deak, M., Ross, F. A., Hawley, S. A., Shpiro, N., Viollet, B., Barron, D., Kemp, B. E., Steinberg, G. R., Hardie, D. G., and Sakamoto, K. (2014) Mechanism of action of compound-13: An alpha1-selective small molecule activator of AMPK. *Chem. Biol.* **21**, 866–879
48. Smith, B. K., Marcinko, K., Desjardins, E. M., Lally, J. S., Ford, R. J., and Steinberg, G. R. (2016) Treatment of nonalcoholic fatty liver disease: Role of AMPK. *Am. J. Physiol. Endocrinol. Metab.* **311**, E730–E740
49. Esquejo, R. M., Salatto, C. T., Delmore, J., Albuquerque, B., Reyes, A., Shi, Y., Moccia, R., Cokorinos, E., Peloquin, M., Monetti, M., Barricklow, J., Bollinger, E., Smith, B. K., Day, E. A., Nguyen, C., *et al.* (2018) Activation of liver AMPK with PF-06409577 corrects NAFLD and lowers cholesterol in rodent and primate preclinical models. *EBioMedicine* **31**, 122–132
50. Ford, R. J., Fullerton, M. D., Pinkosky, S. L., Day, E. A., Scott, J. W., Oakhill, J. S., Bujak, A. L., Smith, B. K., Crane, J. D., Blumer, R. M., Marcinko, K., Kemp, B. E., Gerstein, H. C., and Steinberg, G. R. (2015) Metformin and salicylate synergistically activate liver AMPK, inhibit lipogenesis and improve insulin sensitivity. *Biochem. J.* **468**, 125–132
51. Fritzemeier, K. H., and Kindl, H. (1983) 9,10-Dihydrophenanthrenes as phytoalexins of Orchidaceae. Biosynthetic studies *in vitro* and *in vivo* proving the route from L-phenylalanine to dihydro-m-coumaric acid, dihydrostilbene and dihydrophenanthrenes. *Eur. J. Biochem.* **133**, 545–550
52. Klongkumnuankarn, P., Busaranon, K., Chanvorachote, P., Sritularak, B., Jongbunprasert, V., and Likhitwitayawuid, K. (2015) Cytotoxic and antimigratory activities of phenolic compounds from dendrobium brymerianum. *Evid. Based Complement. Alternat. Med.* **2015**, 350410
53. Bhummaphan, N., Petpiroon, N., Prakhongcheep, O., Sritularak, B., and Chanvorachote, P. (2019) Lusiathridin targeting of lung cancer stem cells via Src-STAT3 suppression. *Phytomedicine* **62**, 152932
54. Cakova, V., Bonte, F., and Lobstein, A. (2017) Dendrobium: Sources of active ingredients to treat age-related pathologies. *Aging Dis.* **8**, 827–849
55. Ou-Yang, S. H., Jiang, T., Zhu, L., and Yi, T. (2018) Dioscorea nipponica makino: A systematic review on its ethnobotany, phytochemical and pharmacological profiles. *Chem. Cent. J.* **12**, 57
56. Pollastro, F., Minassi, A., and Fresu, L. G. (2018) Cannabis phenolics and their bioactivities. *Curr. Med. Chem.* **25**, 1160–1185
57. Toth, B., Hohmann, J., and Vasas, A. (2018) Phenanthrenes: A promising group of plant secondary metabolites. *J. Nat. Prod.* **81**, 661–678
58. Kopietz, F., Alshuweish, Y., Bijland, S., Alghamdi, F., Degerman, E., Sakamoto, K., Salt, I. P., and Goransson, O. (2021) A-769662 inhibits adipocyte glucose uptake in an AMPK-independent manner. *Biochem J.* **478**, 633–646
59. Neumann, D., Woods, A., Carling, D., Wallimann, T., and Schlattner, U. (2003) Mammalian AMP-activated protein kinase: Functional, heterotrimeric complexes by co-expression of subunits in Escherichia coli. *Protein Expr. Purif.* **30**, 230–237
60. Rhein, P., Desjardins, E. M., Rong, P., Ahwazi, D., Bonhoure, N., Stolte, J., Santos, M. D., Ovens, A. J., Ehrlich, A. M., Sanchez Garcia, J. L., Ouyang, Q., Kjolby, M. F., Membrez, M., Jessen, N., Oakhill, J. S., *et al.* (2021) Compound- and fiber type-selective requirement of AMPKgamma3 for insulin-independent glucose uptake in skeletal muscle. *Mol. Metab.* **51**, 101228
61. Patel, K., Foretz, M., Marion, A., Campbell, D. G., Gourlay, R., Boudaba, N., Tournier, E., Titchenell, P., Pegg, M., Deak, M., Wan, M., Kaestner, K. H., Goransson, O., Viollet, B., Gray, N. S., *et al.* (2014) The LKB1-salt-inducible kinase pathway functions as a key gluconeogenic suppressor in the liver. *Nat. Commun.* **5**, 4535